A new Late Holocene sea-level record from the Mississippi Delta: evidence for a climate/sea level connection?

Juan L. González*, Torbjörn E. Törnqvist

Department of Earth and Environmental Sciences, Tulane University, 6823 St. Charles Avenue, New Orleans, LA 70118-5698, USA

ARTICLE INFO

ABSTRACT

A detailed relative sea-level (RSL) record was constructed for the time interval 600–1600 AD, using basal peat to track sea level and containing 16 sea-level index points that capture ∼60 cm of RSL rise. The study area is in the Mississippi Delta where the spring tidal range is ∼0.47 m, the impact of ocean currents on sea-surface topography is limited, and crustal motions are well constrained. Age control was obtained by AMS ^{14}C dating and most ages represent weighted means of two subsamples. Sample elevations were determined by combining differential GPS measurements with optical surveying. All index points were plotted as error boxes using 2σ confidence intervals for the ages, plus all vertical errors involved in sampling and surveying, as well as the indicative range of the samples. A striking clustering of sea-level index points between ∼1000 and ∼1200 AD suggests a possible acceleration in the rate of RSL rise. Removal of the long-term trend (0.60 mm yr^{-1}) allows for the possibility of a sea-level oscillation with a maximum amplitude of ∼55 cm. However, given the size of the error boxes the possibility that oscillations did not occur cannot be entirely ruled out. Comparison of the new RSL record with various proxy climate records suggests that sea level in this area may have responded to hemispheric temperature changes, including the Medieval Warm Period and the Little Ice Age. However, given the error margins associated with this reconstruction, it is stressed that this causal mechanism is tentative and requires corroboration by high-resolution sea-level reconstructions elsewhere.

1. Introduction

One of the most heated topics within the context of global warming is sea-level change. While much of the debate focuses on forecasting sea-level rise, typically with substantial uncertainties given the largely unknown future of the Greenland and Antarctic ice sheets, it is somewhat ironic that the geologically recent history of sea-level change is relatively poorly understood. The commonly accepted view is that the past few thousand years represent a time of high and "relatively stable" sea level. The Intergovernmental Panel on Climate Change (IPCC), for example, states that there was an increase in sea level in the 20th century after a period of little change between 0 and 1900 AD (Bindoff et al., 2007). However, several recent studies (Shaw and Ceman, 1999; Morton et al., 2000; Behre, 2007; Mauz and Bungenstock, 2007; Goodwin and Harvey, 2008) have suggested that sea level has oscillated during the last two millennia, with estimates on the amplitude of these oscillations as high as several meters. No globally consistent pattern has

yet emerged, suggesting that at least some of these fluctuations (if real) are local rather than global. It is important to verify the occurrence and to quantify the magnitude of such oscillations to ascertain whether they are the global sea-level manifestations of century-scale climate episodes such as those that occurred during the Late Holocene. Understanding these sea level/climate relationships of the recent geologic past can provide a valuable context for predictions of future sea-level change.

Several relative sea-level (RSL) studies have been conducted to specifically explore climate/sea level connections over the past 2000 years (Varekamp et al., 1992; Nydick et al., 1995; Varekamp and Thomas, 1998; Van de Plassche et al., 1998; Shaw and Ceman, 1999; Gehrels, 1999; Van de Plassche, 2000; Gehrels et al., 2002, 2005; Donnelly, 2006). All these studies are from the North American side of the Atlantic Ocean, and nearly all employ one of two proxies to track sea-level: marsh foraminiferal assemblages and/or basal peat. In most cases the climate/sea level links are tenuous, which in some instances might be simply explained by the fact that climate records available at the time lacked the resolution to allow a valid comparison. The study by Van de Plassche et al. (1998) stands out for having the highest density of sea-level index points. Their chronology, which extends over a 1400-year-long

* Corresponding author. Tel.: +1 504 862 3274; fax: +1 504 865 5199.
E-mail address: jgonzal6@tulane.edu (J.L. González).

period, is supported by 32 ^{14}C ages, equivalent to approximately one index point per 40 years. Most other RSL histories contain an average of one index point per 80–100 years. In some studies (e.g., Shaw and Ceman, 1999) low index point densities are the result of rejection of large numbers of ^{14}C ages.

Here we present a high-resolution RSL record that spans 1000 years (600–1600 AD) based on 16 sea-level index points (derived after a rigorous screening of an initial data set of 28 index points), equivalent to one data point per ∼60 years on average. The new record is unique in that two ^{14}C age measurements were performed for each index point. Our goal with this new record is to address the following two questions:

1. Is there evidence for sea-level oscillations within this time period? If so, what is the maximum amplitude and duration of such oscillations?
2. If present, are any naturally occurring sea-level oscillations correlative in time with regional to hemispheric paleoclimate records?

2. Study area

This investigation was conducted on the western margin of the Mississippi Delta, Louisiana, USA. The study area is located along the northern edge of coastal wetlands that fringe Vermilion Bay, a large body of water with a direct connection to the Gulf of Mexico. Samples were retrieved along three approximately parallel lines of section that followed roads or trails leading into the wetlands. The three cross sections (Fig. 1) are contained within an area of approximately 16 km^2, about 6–10 km from Vermilion Bay.

The study area is located within a large (>600 km^2), elliptical shaped geologic basin known as the Five Island Syncline, after the

five piercement-type salt domes that represent the most prominent feature in the landscape (Seglund, 1974; AAPG, 2001; Autin, 2002). This northwest to southeast oriented structure formed as a result of salt withdrawal due to the growth of the five diapirs. Seglund (1974) suggested that short and discontinuous normal faults bound the structure, but no geophysical evidence has been presented to confirm the occurrence of these faults. Using a mass balance approach, Bick (2005) estimated the subsidence rate in the Five Island Syncline resulting from salt withdrawal to be on the order of 0.06–0.16 mm yr^{-1} only. Since salt tectonics operates over much longer timescales than the duration of our time series, it is unlikely that any such subsidence would have varied significantly during the relatively short time span covered by our RSL record. Selection of sampling areas was accompanied by an evaluation of available maps and literature (Wallace, 1954; Seglund, 1974; Saucier, 1994; Autin, 2002) to rule out the presence of salt diapirs or major growth faults underneath the sampling sites.

A blend of attributes makes the U.S. Gulf Coast exceptionally favorable for constructing a high-resolution sea-level chronology. The north-central Gulf of Mexico is a microtidal setting with a present-day mean tidal range of ∼40 cm. We assume that the tidal range in the Mississippi Delta has not been significantly different during the Late Holocene. There is no evidence for tidal amplification effects in coastal bays and estuaries (Table 1).

Coastal areas along the northern Gulf of Mexico are not likely influenced by the disturbing effect that ocean currents may have on sea-surface topography. The northern U.S. Gulf Coast is located in the "shadow" of the Loop Current, a branch of the Gulf Stream that enters the Gulf of Mexico forming an intense clockwise flow, variable in position. At one extreme, the Loop Current has an almost direct path just circling the western tip of Cuba. At the other extreme the current extends deep into the Gulf of Mexico but does not reach the continental shelf. It retakes its short configuration by
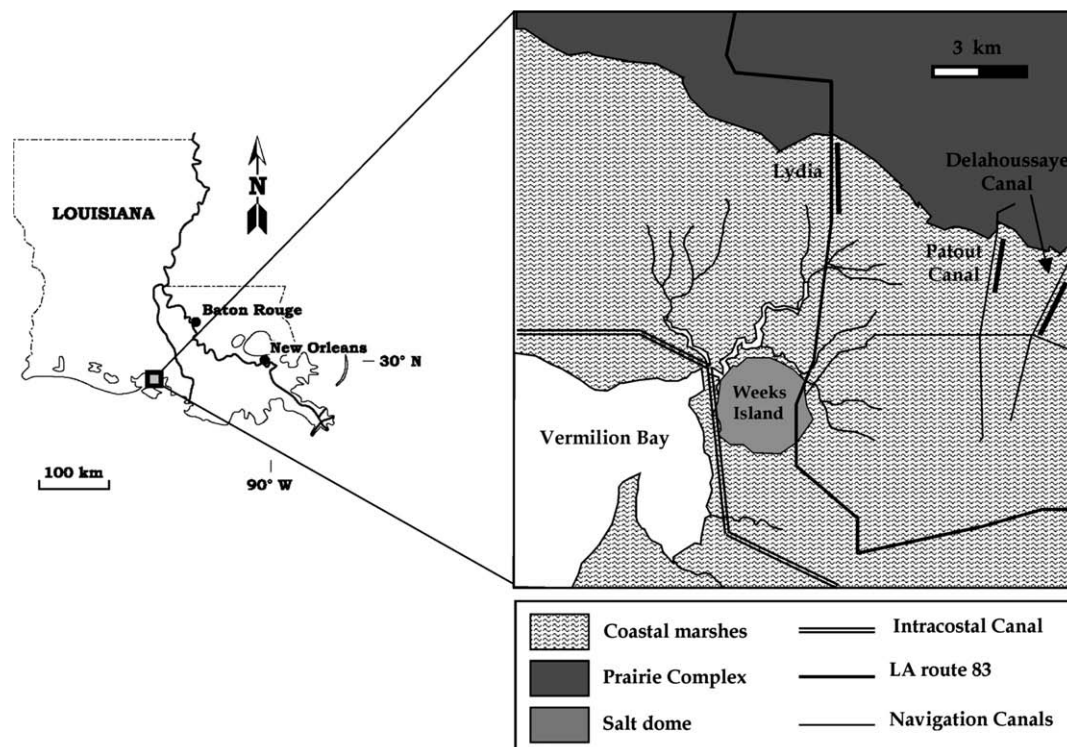
Fig. 1. Location maps. Gray square on the Louisiana state map indicates the location of the study area. The three bold lines on the enlarged map indicate the locations of cross sections.

Table 1
Tidal range at eight NOAA tide gauges in coastal Louisiana.

Tide gauge	Station ID	Latitude N	Longitude W	Mean tidal range (m)	Mean spring tidal range (m)
Calcasieu Pass	8768094	29°45.9′	93°20.6′	0.40	0.60
Freshwater Canal Locks	8766072	29°33.3′	92°18.3′	0.45	0.63
Cypremort Point[a]	8765251	29°42.8′	91°52.8′	0.42	0.52
LAWMA Amerada Pass[a]	8764227	29°26.3′	91°20.2′	0.37	0.52
Port Fourchon	8762075	29°6.8′	90°11.9′	0.37	0.37
Grand Isle	8761724	29°15.8′	89°57.4′	0.32	0.32
Pilot Station SW Pass	8760943	28°55.5′	89°25.1′	0.37	0.37
Shell Beach[a]	8761305	29°52.0′	89°40.3′	0.42	0.46

The average spring tidal range for the eight gauges is 0.47 m.

[a] Tide gauge stations located at the interior of coastal bays and estuaries.

slowly pinching off its extension to form large, warm-core and short-lived eddies that propagate westward. Relative to cooler Gulf of Mexico waters, the Loop Current has a positive sea-surface topographic expression of 20–50 cm (Sturges, 1993).

Lastly, the combined effects of tectonic subsidence and glacio-isostasy, resulting from sediment loading of the lithosphere associated with the building of the Mississippi Delta and from the melting of the Laurentide Ice Sheet respectively, are relatively small in the study area. The long-term rate of RSL rise dominantly reflects glacio-isostasy, and tectonic subsidence only makes a negligible contribution over the time frame of interest here (Törnqvist et al., 2004, 2006; González and Törnqvist, 2006). A higher combined rate of glacio-isostatic adjustment and tectonic subsidence, however, would not preclude filtering out a eustatic signal as our analysis involves the removal of this long-term trend.

Of utmost importance is whether the rates of glacio-isostatic adjustment and tectonic subsidence remained unchanged for the duration of the record. No evidence exists that this is not the case. Postglacial rebound in formerly glaciated areas is characterized by a simple exponential function that indicates decrease in uplift rate with time. Rebound half-lives have been estimated from studies in northern Canada (Andrews, 1968; Dyke et al., 1991) and Fennoscandia (Bakkelid, 1986). The average half-life of rebound in those areas is approximately 2200 years. Assuming a comparable value for the half-life of subsidence in areas of forebulge collapse, such as the northern Gulf of Mexico, and considering that about three half-lives have passed since deglaciation ~7000 cal yr BP, it is argued that over the 1000 years of record in this study the rate of glacio-isostatic adjustment remained essentially constant.

3. Methods

This study relies on basal peat as a tracer of sea level. For about 50 years basal peat has been used as a sea-level indicator in numerous paleo-sea-level studies, mainly in Europe (e.g., Jelgersma, 1961; Van de Plassche, 1982; Denys and Baeteman, 1995; Kiden, 1995; Long et al., 1998; Törnqvist et al., 1998), eastern North America (Redfield and Rubin, 1962; Bloom and Stuiver, 1963; Stuiver and Daddario, 1963; Belknap and Kraft, 1977; Varekamp et al., 1992; Gehrels and Belknap, 1993; Gehrels et al., 1996; Gehrels, 1999; Shaw and Ceman, 1999; Donnelly et al., 2004) and recently along the U.S. Gulf Coast (Törnqvist et al., 2004, 2006).

Formation of basal peat has been explained as resulting from a rise in groundwater level (GWL) (Jelgersma, 1961) and in coastal settings this is recognized as marking the initial flooding of the land by the highest tides during the post-glacial rise in sea level (Redfield and Rubin, 1962). Van de Plassche (1982) established that basal peat formation in coastal settings in the absence of river-gradient effects is confined to an elevation between mean sea level (MSL) and mean high water (MHW); for the Mississippi Delta with its microtidal regime this amounts to only ~20 cm. Van Dijk et al.

(1991) and Cohen (2005) demonstrated that a close relationship between GWL rise and MSL rise exists in the lower portions of the Rhine–Meuse deltaic plain.

The greatest advantage of using basal peat is that the effect of post-depositional compaction, a common source of error in many RSL chronologies, is virtually eliminated. Basal peat commonly accumulates on top of a sloping and highly compacted Pleistocene surface. The consistency of basal peat as a tracer of sea level was highlighted by Shennan and Horton (2002) in an assessment of large numbers of sea-level data from Great Britain.

3.1. Fieldwork

Fieldwork started with extensive exploratory subsurface mapping. Over 130 boreholes were drilled for this purpose, using a 1-m long, 3-cm diameter hand-operated gouge. Although a large area was initially covered, mapping eventually focused on three transects that contain a shallow and laterally continuous basal peat bed. Detailed stratigraphic cross sections were constructed for each transect to aid the selection of sampling sites for basal organic-rich facies.

The Lydia section with 13 sea-level index points spans nearly 0.6 m from 0.30 to 0.87 m below North American Vertical Datum of 1988 (NAVD 88). The neighboring Patout Canal and Delahoussaye Canal sections were added to verify the sea-level trend depicted by the Lydia record. These two sections contain 8 and 7 sea-level index points and cover a narrower depth range (0.29–0.57 and 0.29–0.63 m, respectively). The location of the cross sections is shown in Fig. 1. Undisturbed basal peat samples were obtained using a 6-cm-diameter gouge. The hand drilling approach ensured great accuracy when measuring the depth from which the samples were obtained. All samples were 25 cm long, of which approximately the upper 15 cm was peat and the lower 10 cm was the underlying substrate. The lower boundary of the basal peat was defined in the field by a color change from dominantly brown to dominantly dark gray, the latter corresponding to the buried A-horizon that caps the underlying, consolidated substrate (Törnqvist et al., 2004). In most cases the color transition was striking. Each core was visually inspected for signs of bioturbation or stretching; 12 cores were rejected and redrilled for these reasons.

Elevations of all core sites were obtained by multiple runs of optical surveying from temporary benchmarks using an infrared TOPCON GTS-4B total survey station. Elevations of temporary benchmarks in each of the three study areas were measured relative to National Geodetic Survey (NGS) benchmark AU3428 located southeast of the three areas, using a Differential Global Positioning System (DGPS).[1] The height of benchmark AU3428 with respect to

---

[1] Benchmark AU3428 was also a reference benchmark in the study by Törnqvist et al. (2006) but in that study the benchmark was identified as L043 (the number stamped on the brass plate of the benchmark).

NAVD 88 is +3.16 m. NGS classifies it with a 'C' designation (defined as "may hold, but of the type commonly subject to surface motion"). However, the stability of the benchmark has no effect on the data set since it was only used to provide a reference point for the DGPS survey and any future corrections due to surface motions would apply equally to all samples. The reference benchmark was last surveyed by NGS in January of 1993. Temporary benchmarks and the base station were occupied simultaneously for at least two days (6–8 h per day). After data processing with Trimble Geomatics Office, the network was adjusted with reference to the NAVD 88 orthometric height of benchmark AU3428 and this elevation was propagated through the network using the GEOID 99 model. DGPS data processing was performed by UNAVCO Inc.(Boulder, CO).

3.2. Laboratory work

As a crosscheck of the depth of the A-horizon to basal peat transition as determined in the field, loss on ignition (LOI) analysis was performed at 1 cm intervals for every core. Most color transitions were in good agreement with transitions obtained by LOI. Only in a few cores the transition shifted by up to a few centimeters (González, 2008). Once the depth of the transition was defined, the cores were cut into 1-cm-thick slices; these were then wet sieved over screens with mesh openings of 0.5 and 1.0 mm. When there was a discrepancy between the color and LOI transitions, sampling started at the lower of the two depths and based on the proportion of plant material to silt or clay retained from each slice after sieving, a decision was made on the depth of the transition.

Readily identifiable plant macrofossils (e.g., fruits, seeds), the preferred material for ^{14}C dating, were extremely scarce. Only a limited number of seed fragments were found in some cores, insufficient to obtain reliable ^{14}C ages and of little help in providing paleoenvironmental information. In their absence the chronology is entirely based on herbaceous charcoal; large (>1 cm) charcoal fragments were common. Comparative ^{14}C dating of charcoal and other plant macrofossils (Törnqvist et al., 2004) has shown that herbaceous charcoal usually provides accurate dating results. Some of the largest charcoal fragments were tentatively identified as a robust grass belonging to the genus *Arundinaria*. Plants of this genus generally inhabit low-lying, moist to wet settings of mixed vegetation along stream banks, shrub bogs, sloughs and bayous (Godfrey and Wooten, 1979). Herbaceous charcoal is fragile and it is unlikely to be transported over long distances without fragmenting. Individual charcoal fragments were inspected under the microscope and all younger rootlets were removed. Each charcoal fragment selected was then individually cleaned in an ultrasound bath to remove clay or other amorphous organic material that had adhered to it. Samples were subsequently stored in acidified distilled water at 5 °C.

In the majority of cores, enough datable charcoal was found in the lowermost slice, but in five cases it was necessary to combine material from two adjacent, 1-cm-thick slices, and in one case from three adjacent, 1-cm-thick slices. Most ^{14}C ages were obtained from a single charcoal fragment, but in some instances it was necessary to combine up to six small charcoal fragments. Two subsamples per sample were radiocarbon dated. This provided the means to identify possible inconsistent ages that would have gone undetected with only one age measurement. Double dating of samples also allowed calculating weighted mean ages. A list of all samples dated is presented in Table 2.

3.3. Radiocarbon dating

Radiocarbon dating was carried out by means of accelerator mass spectrometry at the Robert J. Van de Graaff Laboratory,

Utrecht University. We calibrated radiocarbon ages into calendar years with the Groningen CAL25 software (Van der Plicht, 1993) using the INTCAL98 data set (Stuiver et al., 1998). This program offers options such as the use of a smoothed version of the calibration curve and the possibility of calculating the median of the probability distribution of the calibrated radiocarbon age. These are features not found in other calibration packages. We used a smoothing parameter of 40 years, similar to the average of the standard deviations of the ^{14}C ages (see Törnqvist and Bierkens, 1994, for further details). All ages are reported as the 2σ confidence interval of the probability distribution (Table 2). It is important to note that the use of the INTCAL98 data set has virtually no impact on the calibrated ages, as evaluated in a comparison of calibrated ages with the CALIB and OxCal programs (Bronk Ramsey, 1995, 2001; Stuiver et al., 1998) that use the INTCAL04 dataset (González, 2008).

4. Stratigraphy

The stratigraphy in the three cross sections (Lydia, Patout Canal and Delahoussaye Canal) is straightforward (Fig. 2). The depth range for sampling in all three cross sections was within 1.5–2.5 m below the land surface. Basal peat in the Lydia cross section rests on consolidated Peoria Loess capped by an immature paleosol, consisting of a dark gray A-horizon developed in silty material and enriched in highly decomposed organic matter (this paleosol was described by Törnqvist et al. (2004) as an Entisol, suborder Aquent, representing a waterlogged environment; Soil Survey Staff, 1999). In the Patout Canal and Delahoussaye Canal cross sections the peat bed overlies a highly compacted clayey to silty Holocene deposit capped by a similar paleosol. This deposit was mapped in some detail by Törnqvist et al. (2006) who interpreted it as a fluvial overbank deposit of Bayou Teche, the trunk channel belt of the Teche subdelta that became the main distributary of the Mississippi River approximately 4400 ^{14}C years ago (Törnqvist et al., 2006). In the Delahoussaye Canal cross section, the Pleistocene basement with its capping paleosol occurs 2–3 m below the top of the Holocene overbank deposits.

The peat bed sampled along the three lines of section is laterally continuous with a thickness varying between 0.3 and 1.0 m. No indications of prolonged oxidation or pedogenesis were found. Overlying the peat is a 1–2 m thick layer of anthropogenic fill. A gently sloping surface marks the A-horizon to basal peat transition in the Lydia cross section, with an elevation difference of 0.57 m over a distance of 200 m. Throughout the 300-m-long line of section in the Patout Canal area this transition occurs within a topographic depression with a maximum relief of 0.28 m, and in the Delahoussaye Canal area the transition occurs across a low-gradient surface with only 0.34 m of relief over a distance of 330 m.

5. Evaluation of ages

Two aspects of the chronology in this study that warrant attention are the high density of sea-level index points (one per ~60 years on average after a careful assessment of an initially much larger data set, as elaborated upon below), and the dating of two subsamples per index point. The entire data set was rigorously scrutinized for outliers. First the consistency of each pair of subsamples was verified by visual inspection of age vs depth plots for each cross section (Fig. 3). This indicated overall good agreement between most pairs of ages. However, doubts emerged regarding the reliability of samples Lydia IV-1, Lydia XIII-1 and Delahoussaye Canal II-1 given the large age differences between subsamples, ranging from 161 to 411 ^{14}C years (Fig. 3 and Table 2).

Table 2
List of radiocarbon dated samples.

Sample name	UTM coordinate (N)[a]	UTM coordinate (E)[a]	Surface elevation (m)	Depth below surface (m)	δ13C[b] (‰)	14C age[c] (yr BP)	Weighted mean 14C age	Calibrated 2σ age range (yr AD)	Median calibrated age (yr AD)	Laboratory number (UtC-)
Lydia I-1a	3306.730	617.390	1.98	2.31–2.32	−25.2	489 ± 32				12802
Lydia I-1b	3306.730	617.390	1.98	2.31–2.32	−24.9	622 ± 48	530 ± 27	1376–1478	1405	12897
Lydia II-1a	3306.710	617.390	1.55	2.04–2.05	−24.1	893 ± 31				12898
Lydia II-1b	3306.710	617.390	1.55	2.04–2.05	−25.2	899 ± 34	896 ± 23	1074–1202	1145	12803
Lydia III-1a	3306.695	617.390	1.48	2.03–2.05	−25.7	866 ± 31				12899
Lydia III-1b	3306.695	617.390	1.48	2.03–2.05	−25.5	1027 ± 32	944 ± 22	1094–1238	1178	12804
Lydia IV-1a	3306.690	617.390	1.45	1.99–2.01	−24.2	**455 ± 32**				12805
Lydia IV-1b	3306.690	617.390	1.45	1.99–2.01	−24.2	866 ± 34	N/A	1082–1238	1176	12900
Lydia V-1a	3306.670	617.390	1.35	1.95–1.96	−25.2	965 ± 31				12806
Lydia V-1b	3306.670	617.390	1.35	1.95–1.96	−24.6	897 ± 31	931 ± 22	1042–1162	1096	12807
Lydia VI-1a	3306.630	617.390	1.17	1.86–1.87	−25.6	1099 ± 37				12864
Lydia VI-1b	3306.630	617.390	1.17	1.86–1.87	−25.5	1091 ± 35	1095 ± 25	902–994	952	12865
Lydia VII-1a	3306.590	617.390	0.79	1.57–1.58	−24.2	1189 ± 40				12866
Lydia VII-1b	3306.590	617.390	0.79	1.57–1.58	−24.3	1168 ± 35	1177 ± 26	790–930	859	12867
Lydia VIII-1a	3306.570	617.390	0.59	1.43–1.44	−25.1	1391 ± 35				12868
Lydia VIII-1b	3306.570	617.390	0.59	1.43–1.44	−25.2	1511 ± 37	1448 ± 25	570–646	608	12869
Lydia IX-1a	3306.550	617.390	0.58	1.44–1.45	−24.7	1450 ± 35				12870
Lydia IX-1b	3306.550	617.390	0.58	1.44–1.45	−25.0	1498 ± 37	1473 ± 25	550–634	591	12871
Lydia X-1a	3306.744	617.390	1.68	1.98–1.99	−24.1	372 ± 30				13269
Lydia X-1b	3306.744	617.390	1.68	1.98–1.99	−25.0	388 ± 31	380 ± 22	1458–1566	1494	13270
Lydia XI-1a	3306.722	617.390	1.57	1.96–1.97	−24.2	364 ± 28				13271
Lydia XI-1b	3306.722	617.390	1.57	1.96–1.97	−25.4	336 ± 41	355 ± 23	1478–1602	1528	13272
Lydia XII-1a	3306.714	617.390	1.62	2.09–2.10	−26.3	844 ± 31				13273
Lydia XII-1b	3306.714	617.390	1.62	2.09–2.10	−24.6	792 ± 40	824 ± 25	1178–1254	1218	13274
Lydia XIII-1a	3306.620	617.390	0.96	1.76–1.77	−27.3	**1111 ± 34**				13275
Lydia XIII-1b	3306.620	617.390	0.96	1.76–1.77	−24.3	1476 ± 33	N/A	526–642	586	13276
Patout Canal IV-1a	3302.927	622.500	1.39	1.67–1.69	−25.4	255 ± 29				12808
Patout Canal IV-1b	3302.927	622.500	1.39	1.67–1.69	−25.7	335 ± 29	295 ± 21	1534–1646	1616	12809
Patout Canal V-1a	3302.925	622.500	1.40	1.79–1.80	−27.6	918 ± 30				12810
Patout Canal V-1b	3302.925	622.500	1.40	1.79–1.80	−25.4	838 ± 29	877 ± 21	1114–1218	1172	12811
Patout Canal VI-1a	3302.910	622.500	1.37	1.80–1.81	−22.7	862 ± 30				12812
Patout Canal VI-1b	3302.910	622.500	1.37	1.80–1.81	−25.2	940 ± 29	902 ± 21	1070–1190	1138	12813
Patout Canal VII-1a	3302.880	622.490	1.29	1.77–1.78	−24.7	918 ± 32				12814
Patout Canal VII-1b	3302.880	622.490	1.29	1.77–1.78	−25.5	1010 ± 31	965 ± 22	1014–1122	1053	12815
Patout Canal VIII-1a	3302.820	622.490	1.11	1.42–1.43	−26.1	941 ± 32				12816
Patout Canal VIII-1b	3302.820	622.490	1.11	1.42–1.43	−23.5	1025 ± 30	986 ± 23	1002–1082	1032	12817
Patout Canal IX-1a	3302.670	622.470	0.93	1.49–1.50	−25.2	1214 ± 30				12818
Patout Canal IX-1b	3302.670	622.470	0.93	1.49–1.50	−25.4	1176 ± 37	1199 ± 23	770–894	829	12819
Patout Canal X-1a	3302.660	622.470	1.06	1.56–1.58	−24.2	1060 ± 30				12820
Patout Canal X-1b	3302.660	622.470	1.06	1.56–1.58	−25.4	1178 ± 31	1117 ± 22	886–978	932	12821
Patout Canal XI-1a	3302.630	622.460	1.16	1.57–1.58	−26.2	853 ± 32				12822
Patout Canal XI-1b	3302.630	622.460	1.16	1.57–1.58	−25.6	970 ± 32	912 ± 23	1058–1186	1122	12823
Delahoussaye Canal I-1a	3302.020	624.310	1.57	2.04–2.05	−26.2	809 ± 33				12824
Delahoussaye Canal I-1b	3302.020	624.310	1.57	2.04–2.05	−25.2	936 ± 30	879 ± 22	1106–1218	1169	12825
Delahoussaye Canal II-1a	3301.980	624.290	1.48	1.98–2.01	−25.8	959 ± 30				12826
Delahoussaye Canal II-1b	3301.980	624.290	1.48	1.98–2.01	−27.9	**685 ± 31**	N/A	1010–1150	1067	12827
Delahoussaye Canal III-1a	3301.940	624.280	1.85	2.42–2.43	−25.4	840 ± 33				12828
Delahoussaye Canal III-1b	3301.940	624.280	1.85	2.42–2.43	−24.7	866 ± 29	855 ± 22	1150–1234	1194	12829
Delahoussaye Canal IV-1a	3301.840	624.260	1.20	1.81–1.82	−24.1	1065 ± 29				12830
Delahoussaye Canal IV-1b	3301.840	624.260	1.20	1.81–1.82	−25.4	1032 ± 30	1049 ± 21	958–1018	989	12831
Delahoussaye Canal V-1a	3301.790	624.230	0.96	1.58–1.60	−28.4	1016 ± 35				12832
Delahoussaye Canal V-1b	3301.790	624.230	0.96	1.58–1.60	−26.9	1126 ± 32	1076 ± 24	926–1006	969	12833
Delahoussaye Canal VIII-1a	3302.080	624.320	1.60	1.95–1.96	−25.1	879 ± 37				13279
Delahoussaye Canal VIII-1b	3302.080	624.320	1.60	1.95–1.96	−26.0	826 ± 37	853 ± 26	1134–1242	1188	13280
Delahoussaye Canal IX-1a	3302.090	624.340	1.58	1.86–1.87	−25.0	810 ± 50				13277
Delahoussaye Canal IX-1b	3302.090	624.340	1.58	1.86–1.87	−24.7	799 ± 45	804 ± 33	1182–1274	1230	13278

[a] UTM-coordinates (UTM-zone 15R) with reference to North American Datum of 1983 (NAD83).
[b] All ages were obtained from herbaceous charcoal.
[c] 14C ages in bold were rejected.

The largest vertical gap between any two adjacent samples is only 9 cm, which leaves little room for chronological inconsistencies to go unnoticed.

In addition to the visual inspection, the "Sequence" option of OxCal (version 3.10; Bronk Ramsey, 1995, 2001) was used to identify anomalous subsamples. This feature uses Bayesian statistical methods to compare the age distribution of a sample against ages of samples stratigraphically above and below it, and provides an agreement index expressed as a percentage. Low agreement indices characterize ages that are inconsistent with ages immediately above and below. Several runs of the Sequence feature were performed for both the Lydia and Delahoussaye Canal time series (a detailed explanation of the outcomes of this test is given in González, 2008). The best overall agreement was obtained after rejection of the three 14C ages highlighted in Fig. 3 (Lydia IV-1a, Lydia XIII-1a and Delahoussaye Canal II-1b). The combined data set for the three areas consists of 28 sea-level index points; the ages of 25 of these represent weighted means
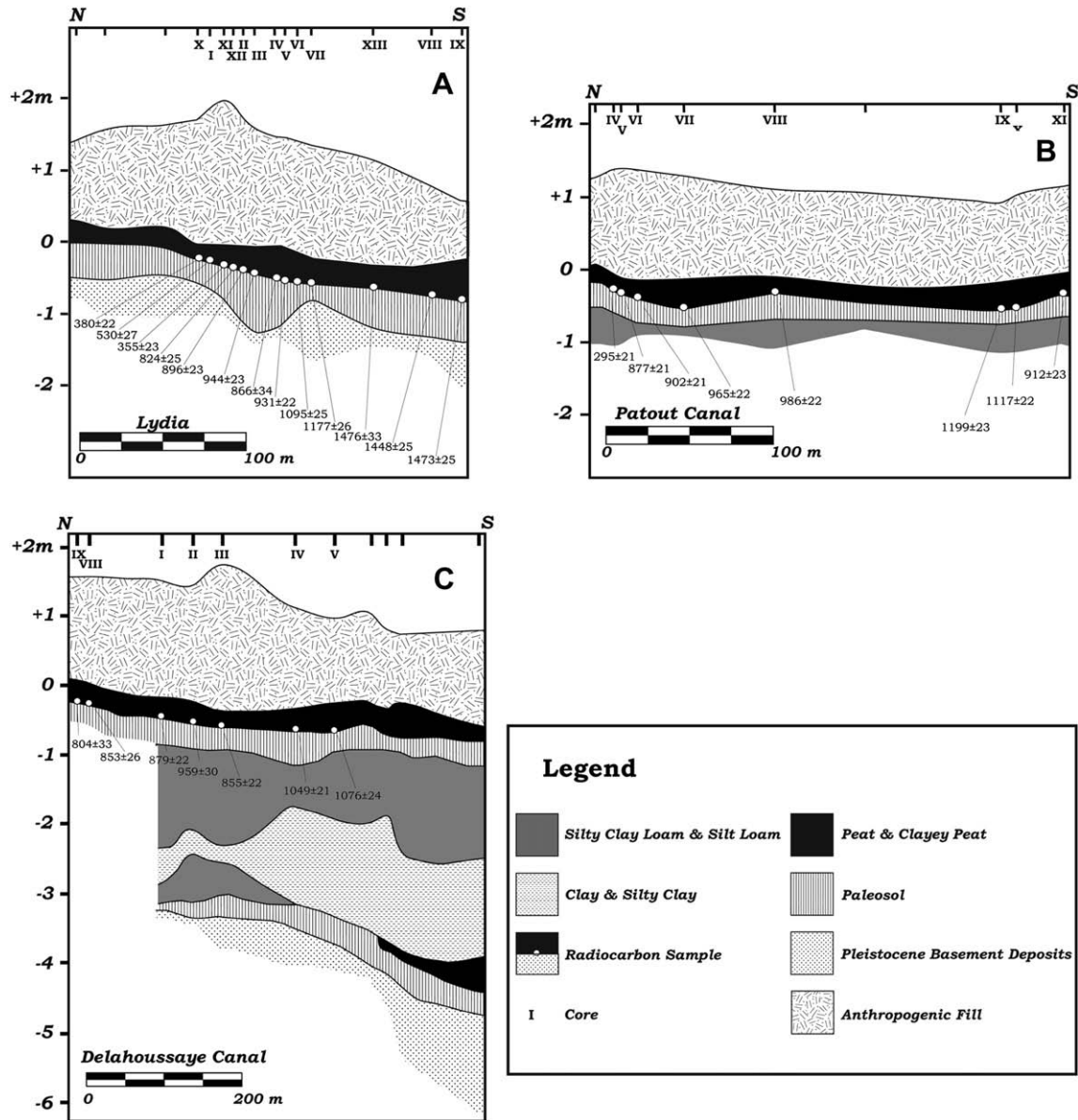
Fig. 2. Stratigraphic cross sections for the sampling areas (A) Lydia, (B) Patout Canal and (C) Delahoussaye Canal. Elevations are with reference to the North American Vertical Datum (NAVD) 88. Sample ages are indicated in ^{14}C yr BP Note the generally straightforward relationship between sample elevation and age.

of the two subsamples, and only three are based on a single age measurement.

6. Error analysis

Error boxes were constructed for each sea-level index point by incorporating the uncertainties associated with the altitudinal and age components of each sample. In this study, given the subtle nature of the sea-level signal that is being targeted, much effort went into minimizing elevation errors. The errors accounted for included those resulting from non-vertical drilling, sampling, optical surveying, and the vertical indicative range of the material dated. Errors associated with DGPS measurements were incorporated only when index points from the three different cross sections were combined. An error of ±1 cm per meter depth was applied to account for non-vertical drilling (e_d); ±2 cm for sampling in the gouge (e_s); ±1 cm for the optical surveys between DGPS-

measured benchmarks and sampling sites (e_os) and ±5 cm for the DGPS measurements (e_gps).

Determining the indicative range (the modern vertical range occupied by a sea-level indicator measured relative to a given tide level) is a challenging step and it can be a major source of error (Kidson, 1982; Van de Plassche, 1986; Gehrels et al., 1996; Horton et al., 2000). A key assumption when using basal peat for sea level reconstructions is that it closely tracks the interval between MSL and MHW. In the absence of botanical remains that would have enabled an assessment of the degree of marine influence on the peat, we present two observations that support that this assumption is likely valid for our study area.

First, the stable carbon isotope signature of the peat provides an approximation of the type of environment in which it accumulated in terms of salinity. Herbaceous marshes in the Mississippi Delta have been subdivided into fresh, intermediate, brackish and saline zones based primarily on vegetation associations (Chabreck, 1972).
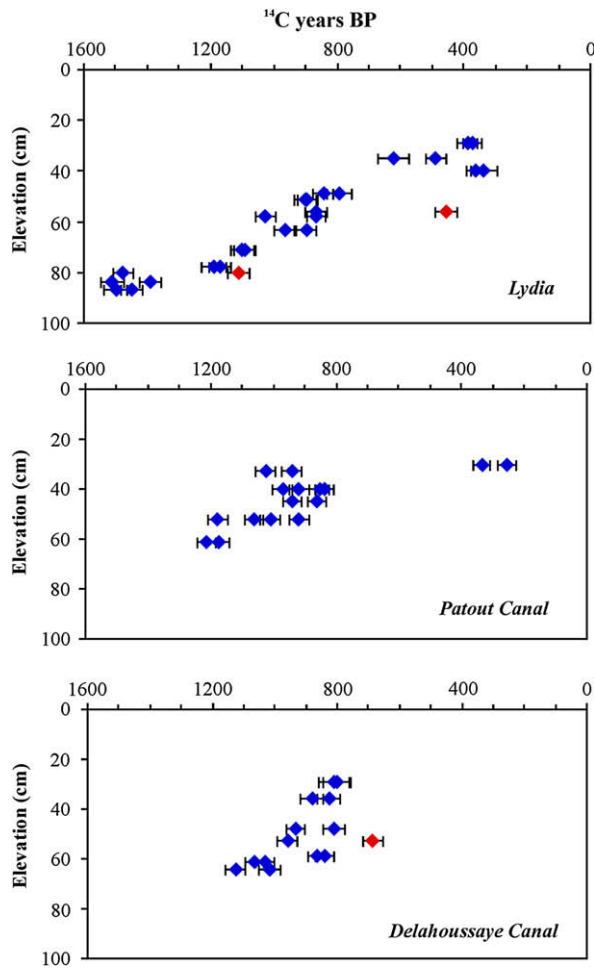
Fig. 3. Plot of uncalibrated radiocarbon ages vs elevation with errors at 1σ levels. Plots include each subsample dated from the three transects. Red diamonds indicate subsamples that have large age differences with their twin subsamples and were ultimately rejected by failing the OxCal Sequence test. Note that most pairs of samples show good mutual agreement. (For interpretation of the references to colour in this figure legend, the reader is referred to the web version of this article.)

Chmura et al. (1987) reported the range of δ^{13}C values for organic carbon-rich sedimentary material for each of these vegetation associations (saline: -18.5 to -14.5‰; brackish: -20.0 to -15.0‰; intermediate: -25.5 to -18.5‰; and fresh: -28.5 to -25.5‰). Most charcoal fragments (41 of 56) used in this study had δ^{13}C values in the range -25.5 to -18.5‰ (Table 2), suggesting vegetation associations that thrive in intermediate salinity conditions (0.3–9.8‰; Chabreck, 1972). This suggest that the marsh received regular inputs of salt water to maintain intermediate salinity conditions, and, thus, that the peat accumulated within the intertidal zone, defined here as the interval between MTL (mean tide level) and MHSW (mean high spring water).

The possibility that charcoal might not be representative of the stable carbon isotope content of the original plant material was considered, but there is evidence indicating that this is unlikely to be the case for our samples. Turney et al. (2006) replicated forest fires and observed that isotopic fractionation of up to ~ 1.3‰ can take place during burning. This fractionation, however, is toward more depleted values and is temperature dependent. It is likely that the δ^{13}C values reported for our samples do not differ much from those of the original plant material, given that fires in coastal marshes do not reach the high temperatures of forest fires. More

importantly, any such a δ^{13}C shift would place our samples more firmly within the intermediate salinity range.

Although the δ^{13}C signature of the peat is used here to argue for a periodic input of salt water in the environment in which the peat formed, and thus to demonstrate marine influence in our samples, we advise that the use of carbon isotope ratios as an indicator or marine influence should be treated with caution in the absence of macro- or microfossil evidence. It should also be noted that to our knowledge no study has as of yet attempted to establish the link between δ^{13}C values of sedimentary organic matter and surface elevation with respect to tide levels along the U.S. Gulf Coast.

Second, water levels in deltaic environments tend to slope very gently in a seaward direction due to a river-gradient effect (Van de Plassche, 1980). Detailed studies of the impact of river gradient on the GWL in the Rhine–Meuse Delta have shown that it only becomes significant at a distance of ~ 50 km upriver from the coast (Van Dijk et al., 1991; Cohen, 2003, 2005). Although this relationship has not been firmly established for the Mississippi Delta, it is likely that this distance is considerably larger given the extremely low gradient of this large river system. The present-day gradient of the lowermost 165 km of the Mississippi River is 1.0 cm km^{-1} (Fig. 4). While the Atchafalaya River has a shorter route to the Gulf of Mexico (about half that of the Mississippi) and a proportionally steeper slope, it is clear that river gradients in this area are very low. Therefore it appears plausible, given the close proximity of the study area to the coast, that river-gradient effects were unlikely to raise local GWL above the intertidal level. Thus, sea level is the dominant control of GWL in the study area.

Considering a present-day spring tidal range along the Mississippi Delta of ~ 47 cm (Table 1) we have adopted a value of ± 12 cm derived from the difference between MTL and MHSW to account for the indicative range (e_{ir}). It should be noted that we applied this value to index points with δ^{13}C signatures indicative of both intermediate salinity and fresh water conditions, but as will be explained below, for the final analysis we excluded those samples that lacked direct isotopic evidence of marine influence.

The total vertical error was calculated by taking the root mean square of the values given for each error following Shennan et al. (2000) and Horton et al. (2000), as follows:

$$\text{Total vertical error} = \sqrt{(e_d)^2 + (e_s)^2 + (e_{os})^2 + (e_{gps})^2 + (e_{ir})^2}$$

The height of the resulting error boxes ranges between 25 and 27 cm (27 and 29 cm when index points from two or three areas are
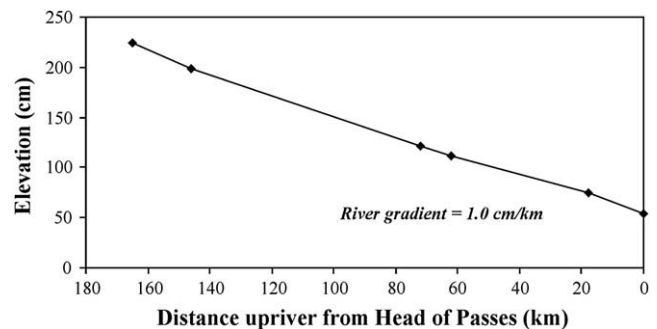
Fig. 4. The Mississippi River gradient plotted between New Orleans and Head of Passes (the site of the first channel bifurcation located 16 km from the mouth), a distance of 165 km. The plot was constructed using daily river stage measurements, where each data point represents the average of over 3700 measurements corresponding to the same days between 1980 and 1999 for which data were available for all gauge stations. For all stations the vertical datum is set to 0 m National Geodetic Vertical Datum of 1929 (NGVD29) which does not correspond to mean sea level. Data provided by the U.S. Army Corps of Engineers New Orleans District (http://www.mvn.usace.army.mil/).

combined and it is necessary to incorporate the DGPS error (e_{gps}) in the calculation). Age errors at the 2σ confidence level of the probability distribution obtained from the calibration of the ^{14}C ages into calendar ages range between 80 and 210 years (Fig. 5).

7. Comparing relative sea-level records from the three areas

When all 28 sea-level index points from the three areas are plotted together, there is a generally good overlap between error boxes from the Lydia and the Delahoussaye Canal cross sections. However, compared to the two neighboring areas, index points from the Patout Canal cross section plot consistently slightly higher (~ 10 cm) (Fig. 5D). We consider the possibility that this offset originates from the fact that the A-horizon to basal peat transition along the Patout Canal transect occurs in a topographic depression, whereas along the Lydia and Delahoussaye Canal cross sections this transition occurs on gently sloping surfaces. A topographic depression could have resulted in water ponding (Jelgersma, 1961) and in a locally raised GWL. However, the possibility that the offset may be related to uncertainties associated with the DGPS measurement of the temporary benchmark used in the Patout Canal area or from paleogeographic changes cannot be entirely ruled out.

The fact that the Patout Canal index points plot consistently higher than index points from the neighboring areas provides important evidence indicating that compaction of the underlying overbank deposits did not occur after peat formation. If post-depositional compaction was significant, index points from the Patout Canal and Delahoussaye Canal areas would plot lower than those from the Lydia area that rest directly on the Pleistocene substrate.

8. Sea-level reconstruction

Due to the slight offset of the Patout Canal data, we perform the following analysis by combining index points from the Lydia and Delahoussaye Canal data sets only. It is important to note that we only use index points indicative of intermediate salinity conditions; under this consideration a total of four index points are left out of the analysis (Lydia III-1 and VI-1, Delahoussaye Canal II-1 and V-1). However, our analysis does include four index points (two from Lydia and two from Delahoussaye Canal) in which only one of the two subsamples provides evidence for intermediate salinity conditions (Table 2). We stress that the only reason to exclude the four fresh water index points is to exercise caution; it does not necessarily mean that they formed above MHSW. First of all, we note that these index points do not plot higher than those that have direct isotopic evidence suggesting periodic saltwater intrusion (Fig. 5A–D). Secondly, sea-level studies in northwest Europe have shown that fresh water index points can closely corroborate sea-level data from coastal-barrier environments.

The new RSL chronology is based on 16 sea-level index points that capture ~ 60 cm of RSL rise. The general RSL trend depicted by the combined Lydia–Delahoussaye Canal data (Fig. 6) suggests the presence of three segments, including a lower gently sloping tail, a steeper middle segment represented by the majority of index points, and a flat upper end.

We first obtained the long-term trend for the full duration of the record by fitting a linear regression through the 16 sea-level index points from the Lydia and Delahoussaye Canal areas (Fig. 6A). The long-term rate of 0.60 mm yr^{-1} primarily reflects glacio-isostatic adjustment (González and Törnqvist, 2006) as tectonic subsidence plays only a minor role in this area. Törnqvist et al. (2006) reported crustal subsidence rates due to sediment loading for the last 8000 years on the order of ~ 0.1 mm yr^{-1} only. Evidence from the Mediterranean (Lambeck et al., 2004) suggests that since the Roman period, ~ 2000 years ago, the eustatic contribution to the long-term sea-level trend (prior to the recent acceleration) has been only on the order of 0.13 ± 0.09 m. We removed the long-term trend from the RSL record in an attempt to isolate any short-term (centennial-scale) eustatic and/or thermosteric fluctuations that might be superimposed on the millennial-scale trend. The residual
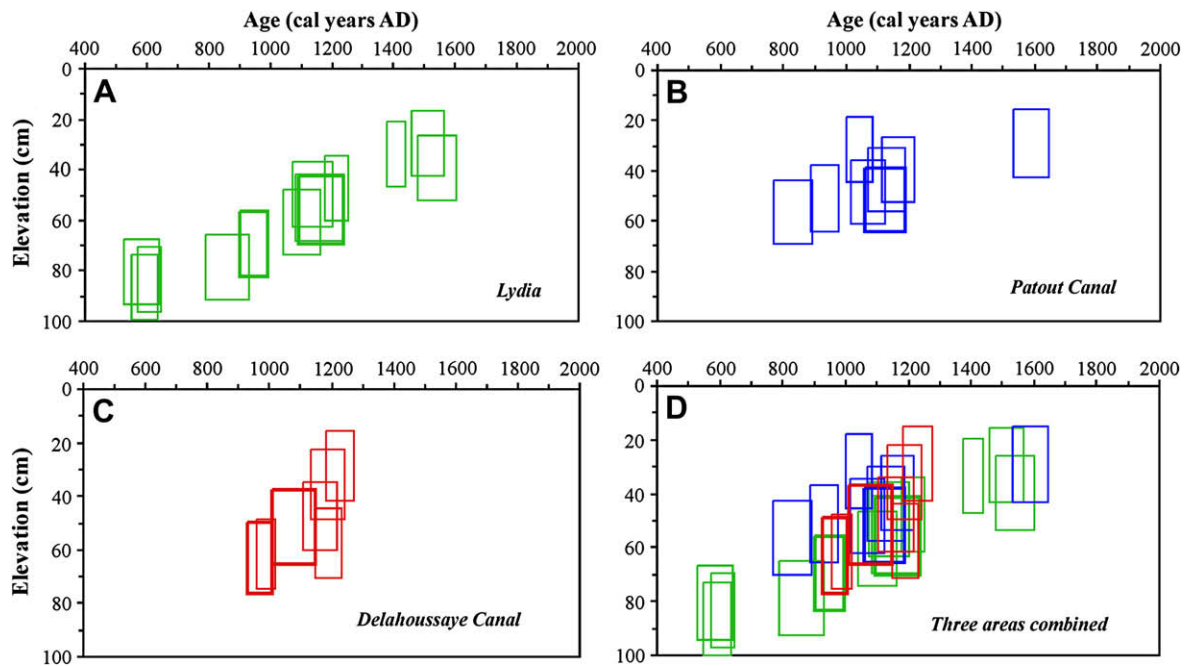
Fig. 5. Age–depth plots of sea-level index points shown as 95% probability error boxes for each of the three transects (A, B, C), and the three transects combined (D). Boxes drawn with bold lines indicate index points where both subsamples have a fresh water isotopic signature. Further explanation in text.
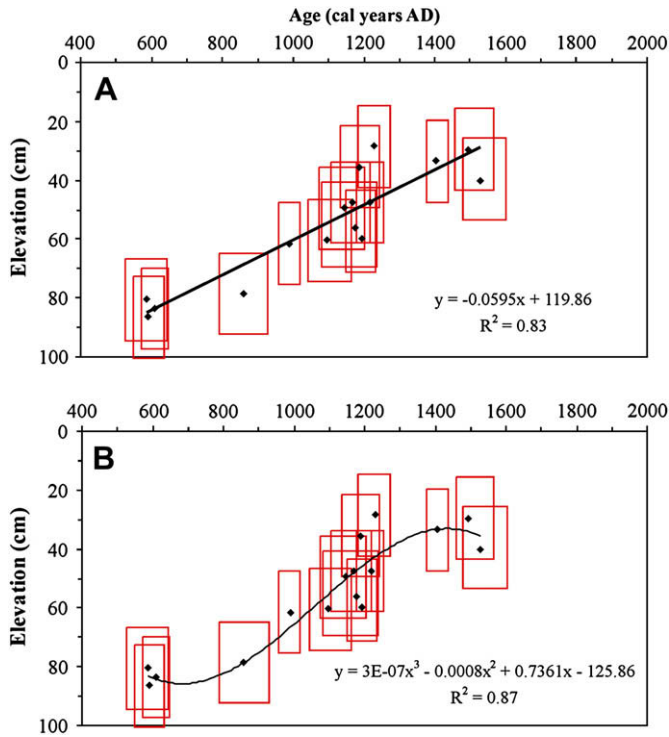
Fig. 6. Linear regression (A) and third order polynomial function (B) fitted through the 16 sea-level index points from the Lydia and Delahoussaye Canal areas with evidence of intermediate salinity. Data points are defined by the median of the calibrated ^{14}C ages plus the elevation of the center of basal-peat samples dated.

signal (Fig. 7) shows that most error boxes overlap the trend line, but around 1200 AD several plot above it. Together with the stacking of error boxes observed between 1000 and 1200 AD in the combined Lydia–Delahoussaye Canal plot (Fig. 6) this allows for the possibility of departures from the long-term trend, which could possibly represent a sea-level oscillation.

Given the visual arrangement of error boxes, we adopt a cubic polynomial function to characterize these data (Fig. 6B). We stress that the purpose of this is merely to facilitate comparison with other proxy records, not to obtain a curve with the best statistical fit. The polynomial function was fitted through the median of the calibrated radiocarbon ages and the elevation center of the basal peat samples.
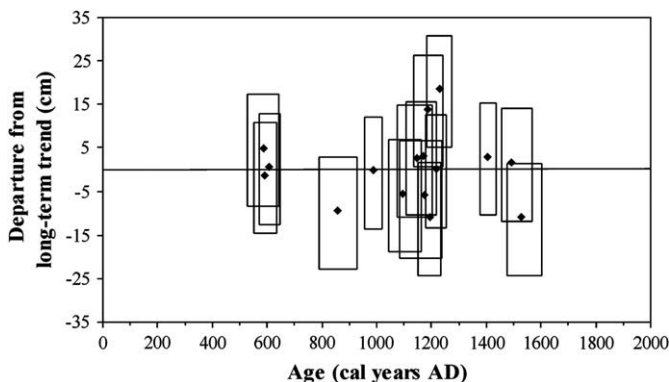
Fig. 7. Plot of detrended 95% probability boxes for the Lydia and Delahoussaye Canal areas. Note the departure of some error boxes from the trend line, around 1200 AD.

9. Have ^{14}C production rates impacted the data analysis?

Gehrels et al. (2005) demonstrated that (sub)centennial-scale fluctuations in salt-marsh sedimentation rates as established by radiocarbon dating may simply be artifacts of the variable production rate of atmospheric [14]C. Thus, we investigated the possibility that plateaus in the radiocarbon calibration curve might have caused the clustering of index points between 1000 and 1200 AD. We used the viewer option of OxCal (Bronk Ramsey, 1995, 2001) to measure the width of the envelope of the INTCAL04 calibration curve between 150 and 1600 ^{14}C years BP. Over this time period the average width of the envelope was found to be 35 calendar years; segments of the curve where the envelope width exceeded 35 years were considered plateaus. In this way seven flat areas of the curve were defined (Fig. 8).

To evaluate the possibility that distortions in the chronology resulted from natural ^{14}C variations we constructed a ^{14}C histogram using the CALHIS program (Stolk et al., 1994). The ^{14}C histogram includes all 56 raw ^{14}C ages (Fig. 8). The impact of variations in atmospheric ^{14}C on the overall shape of the histogram was evaluated by plotting it versus the width of the calibration curve as a function of the ^{14}C time scale. The result supports the notion that the non-linearity of the ^{14}C time scale alone cannot explain the clustering of ^{14}C data. While the highest portion of the intensity peak coincides with low widths of the calibration curve, areas of low intensity in the ^{14}C histogram (for instance in the intervals 550–670 and 1230–1300 ^{14}C yr BP) correspond to some of the widest plateaus.

10. Discussion

Most existing sea-level chronologies lack the data density and the tight controls on elevation to allow extracting a eustatic signal with decimeter-scale amplitude and century-scale duration. The accuracy needed to accomplish this task requires taking the existing methodology (available proxies, dating techniques and elevation measurement techniques) to its performance limit, but even under the best circumstances (ideal physiographic setting and high data density) uncertainties on the order of 20–30 cm remain. We argue that at present no single study can resolve the Late Holocene history of eustatic sea-level change. While new and more accurate proxies become available and significant improvements are made on the accuracy and precision of dating techniques, resolving the eustatic sea-level history for the Late Holocene must depend on replicating results by multiple studies from a wide range of
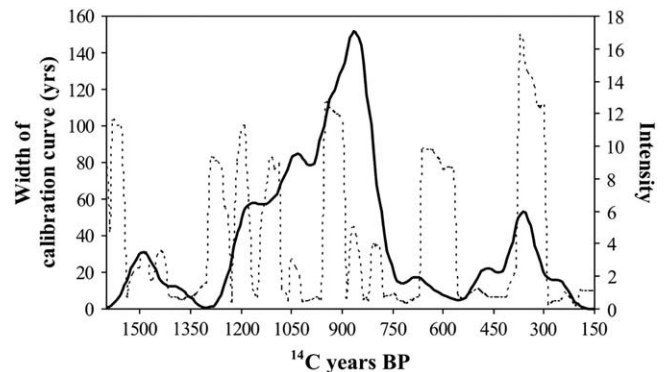
Fig. 8. [14]C histogram (bold line, right axis), constructed with the CALHIS program (Stolk et al., 1994) using all 56 ^{14}C age measurements performed for this study. The width of the calibration curve as measured every 10 years (dashed line, left axis) is also shown. [14]C histograms are obtained by superposition of individual ^{14}C ages, each represented by a Gaussian distribution with the age as the mean value and a width determined by the standard deviation of the ^{14}C measurement.

geographic settings. With these limitations in mind, the present study represents an attempt at resolving the pattern of eustatic change for the time interval from 600 to 1600 AD from the sedimentary archive of the Mississippi Delta, and to seek answers to the two questions formulated in the introduction.

10.1. Is there evidence for sea-level oscillations within this time period? If so, what is the maximum amplitude and duration of such oscillations?

The plot of detrended error boxes from the combined Lydia–Delahoussaye Canal data (Fig. 7) suggests the possibility of non-linear changes in sea level between 600 and 1600 AD. The array of detrended error boxes allows for a possible oscillation with a maximum amplitude of ~55 cm to be captured within it. Conversely, the array of error boxes does not entirely rule out the possibility that no oscillations occurred at all, although this may be a less likely scenario since two of the error boxes plot entirely above the linear trend line around 1200 AD. As pointed out previously, both the Lydia and the Delahoussaye Canal records (Fig. 5A and C) independently suggest a sea-level acceleration around this time.

A number of sea-level studies in the past decade from various localities around the world (Shaw and Ceman, 1999; Morton et al., 2000; Behre, 2007; Mauz and Bungenstock, 2007; Goodwin and Harvey, 2008) have advocated that the last 2000–3000 years witnessed sea-level fluctuations with meter-scale amplitudes. However, two studies from northeastern North America (Van de Plassche et al., 1998; Gehrels et al., 2002) that are recognized for their strong chronologies and their tight vertical control, argue that global sea level merely oscillated centimeters to decimeters on time scales of 100s to ~1000 years over the past 2000 years. Our findings from a different geographic area present additional evidence in support of this latter idea.

The studies by Van de Plassche et al. (1998) and Gehrels et al. (2002) had similar goals (to explore climate/sea level links), contained a high density of index points, and covered roughly the same time interval. However, they are different with respect to their physiographic setting because they were conducted in mid-latitude, formerly glaciated areas (Connecticut and Maine) with a macrotidal regime. They also differ in the type of indicator used to track sea level; they relied on fossil marsh foraminiferal assemblages from non-basal peat, which might not be entirely free of compaction.

Given the substantial errors associated with the three high-resolution sea-level records, we elect not to compare detrended sea-level curves. Instead, we analyze the height of the error envelope for the three reconstructions to set an upper limit for the maximum amplitude that any sea-level oscillations could have had for the period of overlap. Although the general shape of the error envelope for the three reconstructions is markedly different (Fig. 9), they have one thing in common: their maximum height (~60 cm) is similar. Considering the tight controls on the elevation measurements of the three records, we use this number to suggest that if sea level oscillated during this time, the maximum amplitude of any oscillations could not have exceeded 60 cm.

Discrepancies in the overall shape of the error envelopes among the three records can only be partially explained by uncertainties in the chronologies or the elevations measurements. Equally important are external factors which are difficult to detect and preclude distilling a truly eustatic signal. One example already recognized in the North Atlantic is the impact that variations in the strength or position of the Gulf Stream may have had on sea-level change in North America and northwest Europe (Van de Plassche, 2000; Van de Plassche et al., 2003). Other possibilities include gravitational effects due to ice sheet and glacier growth or melt (Mitrovica et al.,
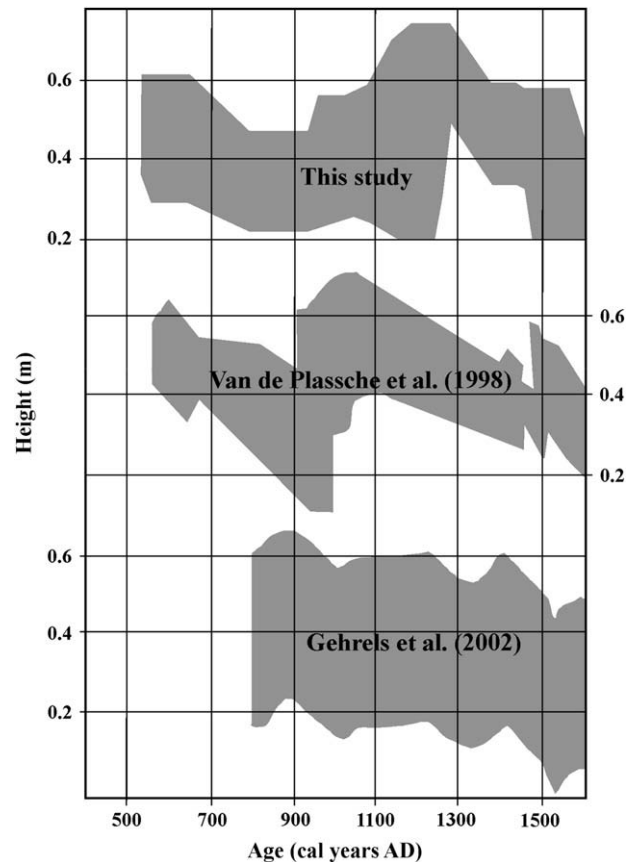
Fig. 9. Comparison of the error envelope for the detrended sea-level record from the present study with those from Maine (Machiasport) (Gehrels et al., 2002) and Connecticut (Van de Plassche et al., 1998). All three error envelopes allow for sea-level oscillations with maximum amplitudes of ~0.6 m.

2001), which may have been a more significant factor in sea-level records from higher latitudes.

10.2. If present, are any naturally occurring sea-level fluctuations correlative in time with regional to hemispheric paleoclimate records?

To assess how the rate of sea-level change may have varied through time and to facilitate comparison with paleoclimate records, we used the derivative of the cubic polynomial function fitted through the data (Figs. 10 and 11). The rationale is that at time scales of 100s of years, variations in the rate of RSL change may result from climatically driven changes in eustasy and thermal expansion, rendering it a potentially sensitive indicator of changes in the mass and volume of the oceans that should have relatively short response times to climate-induced changes. It must be stressed here that this analysis should be considered preliminary, given the magnitude of the errors as discussed previously. However, as shown above, our errors are similar to those of the best currently available studies that have performed similar comparisons with other proxy records. Given that this may remain a limitation of high-resolution sea-level studies for the foreseeable future, we stress once more that the following analysis should be scrutinized by similar studies elsewhere, and that our findings at this stage must be considered preliminary. As expected, the derivative suggests that the highest rates of RSL rise appear to have occurred between ~1000 and 1200 AD. Again, the use of the
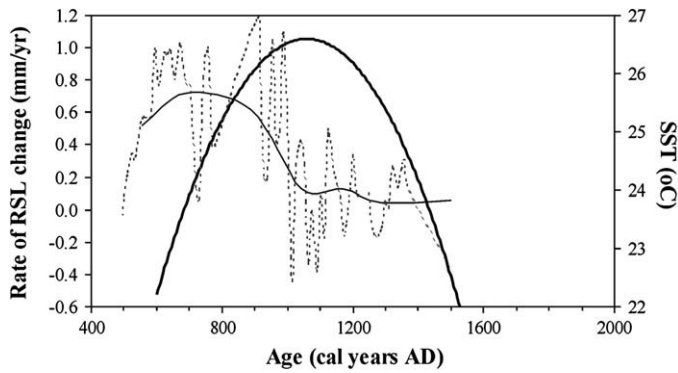
Fig. 10. Rate of RSL change from 600 to 1600 AD (bold line, left axis) compared with a sea-surface temperature record from the northern Gulf of Mexico (Richey et al., 2007) smoothed with a 200 year moving average (thin line, right axis). The dotted line is the high-resolution SST reconstruction.

derivative merely serves for comparison with climate records and not to calculate exact rates of RSL change.

The sea-level response to changes in ocean temperature was explored using a high resolution, 1400-year-long sea-surface temperature (SST) record from the northern Gulf of Mexico (Richey et al., 2007). This record suggests unusually high SST variability of ~3 °C and indicates two multi-decadal intervals between 500 and 900 AD with SSTs as warm as or warmer than near-modern conditions. The SST maxima occurred between 540 and 900 AD, the minima between 1050 and 1650 AD, with the shift towards cooler temperatures around 950 AD (Fig. 10). Since a shift in SST of ~3 °C would impact the thermal structure of the upper water column, comparison with this record aims at a direct examination of the possible thermosteric contribution to sea level in the Gulf of Mexico.

Given the much lower resolution of our record, variations in the rate of RSL change are compared with a smoothed SST record using a 200-year moving average (Fig. 10). A close correspondence of the two curves, or a sea-level response that slightly lags the SST record, was expected. However, the two curves are out of phase and are difficult to reconcile with any known mechanism connecting climate and sea level. This indicates that any sea-level fluctuations as suggested by our record may be the result of phenomena that operate on a larger scale. We therefore next turn to surface air
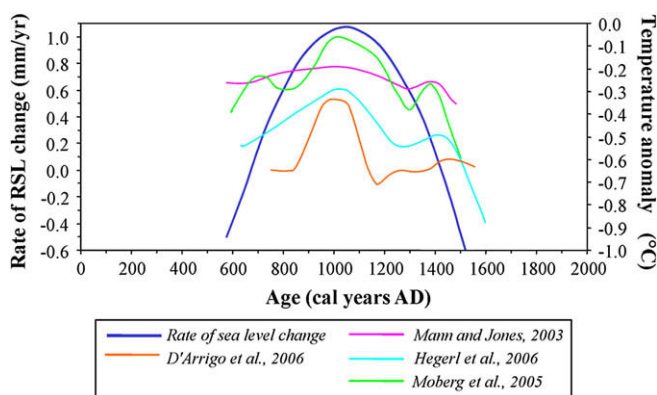
temperature records that are considered to be hemispheric in nature.

A number of high-resolution paleotemperature records are now available for the Northern Hemisphere, but only a few of these records extend beyond the last millennium and lend themselves for comparison with our findings (Mann and Jones, 2003; Moberg et al., 2005; D'Arrigo et al., 2006; Hegerl et al., 2006). These records are based on a variety of climate proxies which ensures that they are robust, and they all have hemispheric significance. Although these time series display important divergences during the past 1000 years there is a reasonably coherent picture featuring the Medieval Warm Period (MWP; ~900 to ~1200 AD), and the Little Ice Age (LIA; ~1400 to ~1900 AD). In terms of the amplitude of temperature variability they depict between MWP and LIA, the Mann and Jones (2003) record suggests <0.5 °C while the reconstructions by Moberg et al. (2005), D'Arrigo et al. (2006) and Hegerl et al. (2006) all indicate ~1 °C.

All temperature records were smoothed with a 200-year moving average (Fig. 11). Comparison of the various records suggests that the increase in the rate of RSL rise from 600 to about 1100 AD coincided with the atmospheric warming that persisted through the MWP. After 1100 AD, the possible deceleration of the rate of RSL rise was concurrent with transitional cooling conditions that led to the early stages of the LIA. Despite the fact that the peak in atmospheric temperatures is recorded at slightly different times by the different reconstructions, they all appear to peak just prior to the peak in the rate of RSL rise centered around 1100 AD. We assume here that coastal marsh peat accumulation did not significantly lag the acceleration in RSL rise (in other words, we cannot entirely rule out a small time lag due to a delayed system response such as has been reported in the literature; Allen, 1995; Kirwan and Murray, 2008). The apparent close match between the rate of RSL change and the hemispheric paleo-temperature records, coupled with the lack of correspondence with the regional SST record suggests that sea level in the Gulf of Mexico may have responded primarily to the hemispheric temperature signal. This, in turn, makes thermal expansion within the Gulf of Mexico a less likely driving mechanism, so we tentatively suggest that the signal may be related to glacio-eustasy.

11. Conclusions

The new Late Holocene sea-level record from the Mississippi Delta features an error envelope around detrended sea-level index points with a maximum height of ~55 cm. This sets an upper boundary for any sea-level oscillations that might have occurred between 600 and 1600 AD. However, we stress that given the error margins, the possibility of a linear trend of RSL rise for the duration of this new record cannot be entirely discarded.

The new data allow for the possibility of an acceleration in the rate of RSL rise during the time interval 1000–1200 AD. The peak in the rate of sea-level rise lags a peak in SST in the Gulf of Mexico by almost 400 years. A much better correspondence may exist between our sea-level record and Northern Hemisphere paleo-temperature records. Increasing atmospheric temperatures leading to and coinciding with the MWP may correspond with a slight acceleration of RSL rise in the Mississippi Delta. The opposite also holds true: cooling temperatures transitional to the LIA may be matched by decreasing rates of RSL rise. The lack of correlation with the SST record for the Gulf of Mexico, and the apparent positive correlation with the atmospheric temperature records for the Northern Hemisphere would favor a glacio-eustatic signature in our sea-level record, rather than regional thermal expansion.

Further elucidating the global sea-level history for the Late Holocene will require the corroboration of these new results by

Fig. 11. Rate of RSL change from 600 to 1600 AD, compared with the low-frequency signal of four surface–air temperature reconstructions for the Northern Hemisphere that overlap in time with the new sea-level record. The temperature records represent anomalies with respect to the 1961–1990 instrumental reference period.

numerous high-resolution studies employing different sea-level indicators and covering widely different geographic settings. We view the present study as a contribution in that direction and stress that our findings must be considered tentative.

Acknowledgments

References

AAPG (American Association of Petroleum Geology), 2001. Gulf of Mexico Basin: Tectonics, Development and Petroleum Systems. Re-Discover Series No 3. CD published by AAPG/Datapages.

Allen, J.R.L., 1995. Salt-marsh growth and fluctuating sea-level: implications of a simulation model for Flandrian coastal stratigraphy and peat-based sea-level curves. Sedimentary Geology 100, 21–45.

Andrews, J.T., 1968. Postglacial rebound in Artic Canada: similarity and prediction of uplift curves. Canadian Journal of Earth Sciences 5, 39–47.

Autin, W.J., 2002. Landscape evolution of the Five Island of south Louisiana: scientific policy and salt dome utilization and management. Geomorphology 47, 227–244.

Bakkelid, S., 1986. The determination of rates of land uplift in Norway. Tectonophysics 130, 307–326.

Behre, K.E., 2007. A new Holocene sea-level curve for the southern North Sea. Boreas 36, 82–102.

Belknap, D.F., Kraft, J.C., 1977. Holocene relative sea-level changes and coastal stratigraphic units on the northwest flank of the Baltimore Canyon Trough geosyncline. Journal of Sedimentary Petrology 47, 610–629.

Bick, S.J., 2005. Quantifying Spatial Variability of Relative Sea-Level Change in the Mississippi Delta. Unpublished MS. Thesis, University of Illinois at Chicago. 47 p.

Bindoff, N.L., Willebrand, J., Artale, V., Gregory, J., Gulev, S., Hanawa, K., Le Quere, C., Levitus, S., Nojiri, Y., Shum, C.K., Talley, L.D., Unnikrishna, A., 2007. Observations: Oceanic climate change and sea level. In: Climate Change 2007: The Physical Science Basis. Contribution of Working Group I to the Fourth Assessment Report of the Intergovernmental Panel on climate Change. Cambridge University Press, Cambridge United Kingdom, pp. 385–432.

Bloom, A.L., Stuiver, M., 1963. Submergence of the Connecticut coast. Science 139, 332–334.

Bronk Ramsey, C., 1995. Radiocarbon calibration and analysis of stratigraphy: The OxCal Program. Radiocarbon 37, 425–430.

Bronk Ramsey, C., 2001. Development of the radiocarbon program OxCal. Radiocarbon 43, 355–363.

Chabreck, R.H., 1972. Vegetation, water and soil characteristics of the Louisiana coastal region. Agricultural Bulletin, 664. Louisiana State University, 89 p.

Chmura, G.L., Aharon, P., Socki, R.A., Abernethy, R., 1987. An inventory of ^{13}C abundances in coastal wetlands of Louisiana, USA: vegetation and sediments. Oecologia 74, 264–271.

Cohen, K.M., 2003. Differential subsidence within a coastal prism. Published PhD thesis, Department of Physical Geography, Utrecht University. Netherlands, Geographical Studies 316, 176 p.

Cohen, K.M., 2005. 3D geostatistical interpolation and geological interpretation of paleo-groundwater rise in the Holocene coastal prism in The Netherlands. In: Giosan, L., Bhattacharya, J.P. (Eds.), River Deltas—Concepts, Models, and Examples. SEPM (Soc. Sediment. Geol.), 83. Special Publication, pp. 341–364.

D'Arrigo, R., Wilson, R., Jacoby, G., 2006. On the long-term context for late twentieth century warming. Journal of Geophysical Research 111, D03103. doi:10.1029/2005JD006352.

Denys, L., Baeteman, C., 1995. Holocene evolution of relative sea-level and local mean high water spring tides in Belgium—a first assessment. Marine Geology 124, 1–19.

Donnelly, J.P., 2006. A revised late Holocene sea-level record for northern Massachusetts, USA. Journal of Coastal Research 22, 1051–1061.

Donnelly, J.P., Cleary, P., Newby, P., Ettinger, R., 2004. Coupling instrumental and geologic records of sea level change: Evidence from southern New England of an increase in the rate of sea-level rise in the late 19th century. Geophysical Research Letters 31, L05203.

Dyke, A.S., Morris, T.F., Green, D.E.C., 1991. Postglacial tectonics and sea-level history of the central Canadian Artic. Geological Survey of Canada Bulletin 397, 1–56.

Gehrels, W.R., 1999. Middle and late Holocene sea-level changes in eastern Maine reconstructed from foraminiferal saltmarsh stratigraphy and AMS C-14 dates of basal peat. Quaternary Research 52, 350–359.

Gehrels, W.R., Belknap, D.F., 1993. Neotectonic history of eastern Maine evaluated from historic sea-level data and ^{14}C dates on salt-marsh peats. Geology 21, 615–618.

Gehrels, W.R., Belknap, D.F., Kelley, J.T., 1996. Integrated high-precision analysis of Holocene relative sea-level changes: lessons from the coast of Maine. Geological Society of America Bulletin 108, 1073–1088.

Gehrels, W.R., Belknap, D.F., Black, S., Newnham, R.M., 2002. Rapid sea level rise in the Gulf of Maine, USA, since AD 1800. The Holocene 12, 383–389.

Gehrels, W.R., Kirby, J.R., Prokoph, A., Newham, R.M., Achterberg, E.P., Evans, H., Black, S., Scott, D.B., 2005. Onset of recent rapid sea-level rise in the western Atlantic Ocean. Quaternary Science Reviews 24, 2083–2100.

Godfrey, R.K., Wooten, J.W., 1979. Aquatic and Wetland Plants of Southeastern United States. Monocotyledons. The University of Georgia Press, 712 pp.

González, J.L, 2008. Exploring the late Holocene sedimentary record of the Mississippi Delta for climate sea-level links. Unpublished PhD. Thesis, Tulane University 156 pp.

González, J.L., Törnqvist, T.E., 2006. Coastal Louisiana in crisis: Subsidence or sea-level rise? Eos Transactions 87, 493–498.

Goodwin, I.D., Harvey, N., 2008. Subtropical sea-level history from coral microatolls in the Southern Cook Islands, since 300 AD. Marine Geology 253, 14–25.

Hegerl, G.C., Crowley, T.J., Hyde, W.T., Frame, D.J., 2006. Climate sensitivity constrained by temperature reconstructions over the past seven centuries. Nature 440, 1029–1032.

Horton, B.P., Edwards, R.J., Lloyd, J.M., 2000. Implications of a microfossil-based transfer function in Holocene Sea level studies. In: Shennan, I., Andrews, J. (Eds.), Holocene Land-Ocean Interactions and Environmental Changes around the North Sea, vol. 166. Geological Society, London, Special Publications, pp. 41–54.

Jelgersma, S., 1961. Holocene sea-level changes in the Netherlands. Mededelingen van de Geologische Stichting, Serie C 6 (7), 1–100.

Kiden, P., 1995. Holocene relative sea-level change and crustal movement in the southwestern Netherlands. Marine Geology 124, 21–41.

Kidson, C., 1982. Sea-level changes in the Holocene. Quaternary Science Reviews 1, 121–151.

Kirwan, M.L., Murray, A.B., 2008. Tidal marshes as disequilibrium landscapes? Lags between morphology and Holocene sea level change. Geophysical Research Letters 35, L24401. doi:10.1029/2008GLO36050.

Lambeck, K., Anzidei, M., Antonioli, F., Benini, A., Esposito, A., 2004. Sea level in Roman time in the central Mediterranean and implication for recent change. Earth and Planetary Science Letters 224, 563–575.

Long, A., Innes, J.B., Kirby, J.R., Lloyd, J.M., Rutherford, M.M., Shennan, I., Tooley, J.M., 1998. Holocene sea-level change and coastal evolution in the Humber estuary, eastern England: an assessment of rapid coastal change. The Holocene 8, 229–247.

Mann, M.E., Jones, P.D., 2003. Global surface temperatures over the past two millennia. Geophysical Research Letters 30 (15), 1820.

Mauz, B., Bungenstock, F., 2007. How to reconstruct trends of late Holocene relative sea level: A new approach using tidal clastic sediments and optical dating. Marine Geology 237, 225–237.

Mitrovica, J.X., Tamisiea, M.E., Davis, J.L., Milne, G.A., 2001. Recent mass balance of polar ice sheet inferred from patterns of global sea-level change. Nature 409, 1026–1029.

Moberg, A., Sonechkin, D.M., Holmgren, K., Datsenko, N.M., Karlén, W., 2005. Highly variable Northern Hemisphere temperatures reconstructed from low and high-resolution proxy data. Nature 433, 613–617.

Morton, R.A., Paine, J.G., Blum, M.D., 2000. Response of stable bay-margin and barrier-island systems to Holocene sea-level highstands, western Gulf of Mexico. Journal of Sedimentary Research 70, 478–490.

Nydick, K.R., Bidwell, A.B., Thomas, E., Varekamp, J.C., 1995. A sea-level rise curve from Guilford, Connecticut, USA. Marine Geology 124, 137–159.

Redfield, A.C., Rubin, M., 1962. The age of salt marsh peat and its relations to recent change in sea-level at Barnstable, Massachusetts. Proceedings of the National Academy of Sciences USA 48, 1728–1735.

Richey, J.N., Poore, R.Z., Flower, B.P., Quinn, T.M., 2007. 1400 yr multiproxy record of climate variability from the northern Gulf of Mexico. Geology 35, 423–426.

Saucier, R.T., 1994. Geomorphology and Quaternary Geologic History of the Lower Mississippi Valley. Mississippi River Commission, Vicksburg, 364 pp.

Seglund, J.A., 1974. Collapse-fault systems of Louisiana Gulf Coast. The American Association of Petroleum Geologist Bulletin 58, 2389–2397.

Shaw, J., Ceman, J., 1999. Salt-marsh aggradation in response to late-Holocene sea level rise at Amherst Point, Nova Scotia, Canada. The Holocene 9, 55–74.

Shennan, I., Horton, B., 2002. Holocene land-and sea-level changes in Great Britain. Journal of Quaternary Sciences 17, 511–526.

Shennan, I., Lambeck, K., Horton, B.P., Innes, J.B., Lloyd, J.M., McArthur, J.J., Purcell, T., Rutherford, M.M., 2000. Late Devesian and Holocene records of relative sea level changes in northwest Scotland and their implications for glacio-hydro-isostatic modelling. Quaternary Science Reviews 19, 1103–1136.

Soil Survey Staff, 1999. Soil taxonomy, a basic system of soil classification for making and interpreting soil surveys. United Sates Department of Agriculture, Natural Resources Conservation Service, Washington, 871 pp.

Stolk, A.D., Törnqvist, T.E., Hekhuis, K.P.V., Berendsen, H.J.A., Van der Plicht, J., 1994. Calibration of ^{14}C histograms: A comparison of methods. Radiocarbon 36, 1–10.

Stuiver, M., Daddario, J.J., 1963. Submergence of the New Jersey coast. Science 142, 451.

Stuiver, M., Reimer, P.J., Bard, E., Beck, J.W., Burr, G.S., Hughen, K.A., Kromer, B., McCormac, G., Van der Plicht, J., Spurk, M., 1998. INTCAL98 radiocarbon age calibration, 24,000–0 cal BP. Radiocarbon 40, 1041–1083.

Sturges, W., 1993. The annual cycle of the Western Boundary current in the Gulf of Mexico. Journal of Geophysical Research 98, 18053–18068.

Törnqvist, T.E., Bierkens, M.F.P., 1994. How smooth should curves be for calibrating radiocarbon ages? Radiocarbon 36, 11–26.

Törnqvist, T.E., Van Ree, M.H.M., Van 't Veer, R., Van Geel, B., 1998. Improving methodology for high-resolution reconstruction of sea-level rise and neotectonics by paleoecological analysis and AMS ^{14}C dating of basal peats. Quaternary Research 49, 72–85.

Törnqvist, T.E., González, J.L., Newsom, L.A., Van der Borg, K., De Jong, A.F.M., Kurnik, C.W., 2004. Deciphering Holocene sea-level history on the U.S. Gulf Coast: A high-resolution record from the Mississippi Delta. Geological Society of America Bulletin 116, 1026–1039.

Törnqvist, T.E., Bick, S.J., Van der Borg, K., De Jong, A.F.M., 2006. How stable is the Mississippi Delta? Geology 34, 697–700.

Turney, C.S.M., Wheeler, D., Chivas, A.R., 2006. Carbon isotope fractionation in wood during carbonization. Geochimica et Cosmochimica Acta 70, 960–964.

Van de Plassche, O., 1980. Holocene water-level changes in the Rhine-Meuse delta as a function of changes in relative sea-level, local tidal range, and river gradient. Geologie en Minjbouw 59, 343–351.

Van de Plassche, O., 1982. Sea-level change and water-level movements in the Netherlands during the Holocene: Mededelingen Rijks Geologische Dienst 36, 1–93.

Van de Plassche, O., 1986. Introduction. In: Van de Plassche, O. (Ed.), Sea-Level Research: A Manual for the Collection and Evaluation of Data. Geo Books, Norwich, pp. 1–26.

Van de Plassche, O., 2000. North Atlantic Climate-Ocean variations and sea level in Long Island sound, Connecticut, since 500 cal yr AD. Quaternary Research 53, 89–97.

Van de Plassche, O., van der Borg, K., de Jong, A.F.M., 1998. Sea-level climate correlations during the past 1400 yr. Geology 26, 319–322.

Van de Plassche, O., van der Schrier, G., Weber, S.L., Gehrels, W.R., Wright, A.J., 2003. Sea-level variability in the northwest Atlantic during the past 1500 years: A delayed response to solar forcing? Geophysical Research Letters 30. doi:10.1029/2003GL017558.

Van der Plicht, J., 1993. The Groningen radiocarbon calibration program. Radiocarbon 35, 231–237.

Van Dijk, G.J., Berendsen, H.J.A., Roeleveld, W., 1991. Holocene water level development in the Netherlands' river area; implications for sea-level reconstruction. Geologie en Mijnbouw 70, 311–326.

Varekamp, J.C., Thomas, E., 1998. Climate change and the rise and fall of sea-level over the millennium. EOS Transactions. American Geophysical Union 69, 74–75.

Varekamp, J.C., Thomas, E., Van de Plassche, O., 1992. Relative sea-level rise and climate change over the last 1500 years. Terra Nova 4, 293–304.

Wallace, W.E., 1954. Fault map of south Louisiana. Transactions of the Gulf Coast Associations of Geological Societies 7, 240.